IEEE Access
Multidisciplinary | Rapid Review | Open Access Journal

Received October 2, 2019, accepted November 3, 2019, date of publication November 7, 2019, date of current version November 20, 2019.

Digital Object Identifier 10.1109/ACCESS.2019.2952188

An Algorithm Based on Sparse Decomposition for Estimating Harmonic and Interharmonic Components of Stationary Signals in Power Systems

TATIANA DE ALMEIDA PRADO[1], ANDRÉA MACARIO BARROS[1], AND GIOVANNI ALFREDO GUARNERI[2]

[1]Graduate Program in Electrical Engineering, Universidade Tecnológica Federal do Paraná (UTFPR), Câmpus Pato Branco 85503-390, Brazil
[2]Department of Electrical Engineering, Universidade Tecnológica Federal do Paraná (UTFPR), Câmpus Pato Branco 85503-390, Brazil

Corresponding author: Andréa Macario Barros (barros@alunos.utfpr.edu.br)

This work was supported in part by the Coordenação de Aperfeiçoamento de Pessoal de Nível Superior—Brasil (CAPES) under Grant 001, in part by the UTFPR, in part by the CAPES, in part by the Fundação Araucária, in part by the Financiadora de Inovação e Pesquisa (FINEP), and in part by the Conselho Nacional de Desenvolvimento Científico e Tecnológico (CNPq).

ABSTRACT Many methods for estimating frequency components of stationary signals in power systems are based on the Discrete Fourier Transform. These methods have a fixed frequency resolution which depends on the sampling frequency and the number of samples of the signal, making it difficult to estimate interharmonics. This paper presents an algorithm for estimating harmonics and interharmonics of power system signals using the signal sparse decomposition technique with an overcomplete dictionary. Discrete Trigonometric Transforms have been analyzed for building this dictionary. The l-fold method has also been applied to the dictionary, which has allowed the adjustment of the frequency grid of the output spectrum. The algorithm proposed is called Harmonics and Interharmonics components Estimation based on Signal Sparse Decomposition, and it was assembled using a dictionary formed by atoms of Discrete Cosine and Discrete Sine Transforms of type II. Three synthetic signals containing harmonic and interharmonics distortions with different noise conditions were used to test the algorithm. The proposed method presented better results in the estimation of harmonic and interharmonics than Discrete Fourier Transform, Matrix Pencil Method and Fast Matching Pursuit algorithms. The results demonstrated robustness to noise and adequate estimation of the interharmonics when the frequency grid is adjusted correctly.

INDEX TERMS Discrete trigonometric transform, harmonics and interharmonics estimation, overcomplete dictionary, power quality signal analysis, signal sparse decomposition.

I. INTRODUCTION

Harmonics and interharmonics disturbances in electrical systems increase as new electronic power devices are connected to the power system [1]. The time-varying, switching circuits, static converters, frequency inverters for speed adjustment of motors, electric-arc furnaces, and other asynchronous pulsed loads generate these distortions [2]. The integer multiples of the power system fundamental frequency are the harmonic components, while interharmonics are those components in fractional multiples of the fundamental frequency [3]. The existence of harmonic components leads to the thermal overheating effect on energy conductors, decreasing the lifetime of electrical appliances and causing interferences in AC grid systems [4]. In turn, the interharmonics components generate effects such as flickering in lighting systems and computer monitors, sub-synchronous oscillations, and voltage fluctuations [1], [2], [5].

Currently, IEC 61000-4-7 defines the methodology for estimating harmonics and interharmonics in power systems [6]. This standard establishes that the voltage and current of an electric system must be sampled using 200 ms windows (12 full cycles at 60 Hz or 10 at 50 Hz). These sampled signals are processed by the Discrete Fourier Transform (DFT), which calculates the energy of the signal's frequency components and makes the estimation of harmonics and

The associate editor coordinating the review of this manuscript and approving it for publication was Eklas Hossain.

interharmonics possible. The frequency resolution obtained using the DFT under the conditions imposed by the standard is 5 Hz, which corresponds to the inverse of the time window's size. Only the frequency components multiples of 5 Hz are correctly identified and the set of the detectable frequency components is called *grid of frequencies* for the DFT. When some frequency components do not correspond precisely to any element in the grid, the DFT algorithm causes a scattering of the energy for these components to adjacent frequencies on the grid, this phenomenon is known as the *spectrum leakage* [2]. The *picket-fence* effect is another phenomenon which occurs when grid resolution limits the detection of components in specific frequencies [7]. These effects prevent the precise identification of frequency components which are not multiples of 5 Hz. However, the grouping methods proposed in IEC 61000-4-7 [6] guarantee that the total energy of harmonics and interharmonics components is estimated accurately. The proper identification of these components enables the design of filters for interharmonic compensation and flicker mitigation [8], [9]. In [10], Lin proposes an algorithm for harmonics and interharmonics estimation based on grouping methods. However, this algorithm cannot estimate correctly adjacent harmonics and interharmonics.

Several methods for estimating individually interharmonic components are proposed in the literature. An algorithm called *Dispersed Energy Distribution* (DED) has been proposed by [1]. This method allows estimating the interharmonics components apart, by calculating the frequency deviation according to the energy distribution in the spectrum. The *Multi-interharmonic Spectrum Separation and Measurement* (MSSM) method, proposed in [11], does an asynchronous sampling of the signal so that all its components are treated as interharmonics. This method identifies peaks in the spectrum obtained by DFT, separates the spectral content for each peak and estimates the parameters of each component.

The *Variational Mode Decomposition* (VMD) technique is also used to decompose power system signals in frequency components [12]. This technique separates the input signal into a discrete number of sub-signals with sparse characteristics, by assuming that each sub-signal is compact around a central frequency [13]. The main advantage of this method is its ability to detect interharmonics and to estimate time-varying spectral components. However, it is necessary to define parameters such as bandwidth and the number of frequency components to be extracted from the signal.

The method presented in [5] uses an optimization algorithm known as *Firefly Algorithm* (FA) to estimate the initial parameters applied to the *Recursive Least Square* (RLS) algorithm, which evaluates amplitudes and phases of the time-varying signal adaptively. Despite presenting adequate results, the FA-RLS algorithm has limited precision, and the definition of the parameters is a challenge in the case of time-varying signals.

Recently, a method based on the solution of a generalized eigenvalue using *Matrix Pencil Method* (MPM) has been proposed in [14]. MPM is similar to Prony's method, but less sensitive to noise [15]. MPM can estimate the frequency, amplitude and relative phase of the frequency components present in a power system signal, regardless of a fixed frequency grid, and responding appropriately to noisy signals with about 25 dB of SNR. Furthermore, MPM is capable of estimating damping coefficients and voltage drops. However, this method has a high computational load in the order of $\mathcal{O}(N^3)$, where N is the number signal samples.

In the last decade, numerous applications in signal processing have used the *Sparse Signal Decomposition* (SSD) technique with *Overcomplete Hybrid Dictionary* (OHD) for detection and classification of modulated signals [16], analysis of ultrasound signals [17], [18], automatic target recognition in radar images [19], denoising and analysis of biomedical signals as electrocardiogram (ECG) [20], [21] and electroencephalogram (EEG) [22], among others. In the analysis of signals in power systems, [23] presents a study for compression and denoising of signals with power quality disturbances, while [24] does the detection and classification of these disturbances. Both use an overcomplete dictionary formed by three matrices: one of unitary impulses delayed in time, one generated by *Discrete Cosine Transform* (DCT) and another generated by *Discrete Sine Transform* (DST). The method has presented better performance in the tests carried out when compared to the *Wavelet Transform* (WT) and DCT methods. However, [23] and [24] do not justify the choice of DCT-II and DST-II to compose the OHD. Moreover, coefficients are not compensated, which leads to inaccurate results once samples are time-shifted by a half sampling time.

Another recent method based on SSD is the Fast Matching Pursuit (FMP) presented by [25]. This method identifies harmonics and interharmonics components using an iterative decomposition based on Matching Pursuit with an overcomplete sinusoidal dictionary. Firstly, FMP finds an approximated frequency by Fast Fourier Transform (FFT) and relates it with the dictionary. Then, an optimization algorithm is applied to estimate the actual phase and frequency of the signal. The FMP method proved to be insensitive to spectral leakage. However, [25] does not set a tolerance limit, and for a small value the algorithm extracts nonexistent harmonic and interharmonics components of the signal.

This work proposes a new algorithm for estimating harmonics and interharmonics components in signals acquired from power systems. The proposed algorithm is based on the SSD technique using an overcomplete dictionary compounded by DCT and DST matrices. The different types of DCT and DST are presented, and their characteristics regarding the decomposition of signals with harmonic distortion are discussed. This discussion is important to justify the choice of the pair DCT-II and DST-II to form the OHD adopted in the proposed algorithm. This algorithm is called *Harmonics and Interharmonics components Estimation based on Signal Sparse Decomposition* (HIESSD). The overcomplete dictionary was assembled using an l-fold overcomplete system [26]. It makes possible to get a finer frequency resolution than by the DFT algorithm, which is 5 Hz considering the

acquisition criteria set out in IEC 61000-4-7 [6]. The HIESSD algorithm estimates the amplitude, phase, and frequency of harmonics and interharmonic components individually with a frequency resolution of up to 0.5 Hz from signals collected in 200 ms sampling windows. We have also evaluated the efficacy of the HIESSD method with acquisition windows smaller than defined in IEC 61000-4-7, of up to 125 ms (7.5 cycles of the fundamental frequency).

The purpose of this work is to present the feasibility of developing an algorithm based on SSD for the estimation of harmonics and interharmonics components, comparing its performance against the DFT, MPM and FMP algorithms with simulated signals containing these harmonic components and with the addition of Gaussian noise. Thus, in this work, tests with real signals obtained in power systems will not be performed. We are also not considering possible deviations from the fundamental frequency that exist in real electrical systems. The current version of HIESSD algorithm is intended for off-line analysis of stationary signals.

In Section II are presented the SSD technique, the different kinds of dictionaries built from harmonic bases, the construction of an OHD using *Discrete Trigonometric Transforms* (DTT) and the l-fold system, and the HIESSD for harmonics and interharmonics estimation. Section III presents the analysis of compound dictionaries by even DTTs and demonstrates the application of the HIESSD method to synthetic signals containing harmonic and interharmonic distortions. The results are compared with the DFT, MPM and FMP methods. In Section IV, the conclusions and future works are presented.

II. METHOD

The signals with harmonic and interharmonic distortions are characterized by the limited number of frequency components and can be represented sparsely in the frequency domain. This feature makes this problem ideal for applying SSD using an OHD consisted of harmonic bases. This section describes the detailing of the SSD technique; the reasonable harmonics bases to compose the OHD; the dictionary construction and; the HIESSD algorithm proposed to estimate harmonics and interharmonics components.

A. SPARSE SIGNAL DECOMPOSITION

SSD is an atomic decomposition technique that seeks to represent arbitrary signals with as few coefficients as possible. In this regard, it is necessary to use a dictionary, which consists of a library of simple waveforms called *atoms*. Accordingly, a linear combination of suitably selected atoms from a dictionary $\Phi \in \mathbb{R}^{N\times M}$ may represent any discrete-time signal $\mathbf{x} \in \mathbb{R}^N$ [27], as shown by Eq. (1):

$$\mathbf{x} = \sum_{m=1}^{M} \boldsymbol{\alpha}_m \boldsymbol{\phi}_m = \Phi\boldsymbol{\alpha}, \tag{1}$$

where $\boldsymbol{\alpha} \in \mathbb{R}^M$ is the vector of sparse coefficients resulting from the signal decomposition, $\boldsymbol{\alpha}_m$ is a coefficient of the vector $\boldsymbol{\alpha}$ and, $\boldsymbol{\phi}_m$ corresponds to an atom in the dictionary.

If $M = N$ and the atoms are orthogonal, the dictionary represents a transformation basis (Fourier, *Wavelet*, DCT, and others) and is said to be *complete*. However, when $M > N$, the dictionary presents non-orthogonal atoms, which contains redundant information. This redundancy brings robustness to the decomposition process. Dictionaries in this category are called *overcomplete*.

The operation to estimate the coefficients $\boldsymbol{\alpha}$ from the signal $\mathbf{x}$ using the dictionary Φ is called *atomic decomposition* and may be treated as an optimization problem represented by Eq. (2):

$$\hat{\boldsymbol{\alpha}} = \min_{\boldsymbol{\alpha}} \|\boldsymbol{\alpha}\|_0 \quad \text{subject to } \mathbf{x} = \Phi\boldsymbol{\alpha}, \tag{2}$$

where $\|\cdot\|_0$ is the norm ℓ_0 which counts nonzero elements in a vector [28]. In the case of signals contaminated with noise, the problem of Eq. (2) can be relaxed to:

$$\hat{\boldsymbol{\alpha}} = \min_{\boldsymbol{\alpha}} \|\boldsymbol{\alpha}\|_0 \quad \text{subject to } \|\mathbf{x} - \boldsymbol{\Phi}\boldsymbol{\alpha}\|_2 \leq \epsilon, \tag{3}$$

where $\epsilon > 0$ represents an error tolerance [28].

In the case of an overcomplete dictionary, the system of equations $\mathbf{x} = \boldsymbol{\Phi}\boldsymbol{\alpha}$ is underdetermined and presents infinite solutions. The solution to this optimization problem is *NP-hard* because it is difficult to find the most sparse representation [27]. The solution can be obtained by approximation methods that refine the current estimate of the vector of sparse coefficients iteratively, modifying those that would bring about significant improvements in signal approximation [28]. There are several methods to solve the problem of Eq. (3). We have chosen the *Orthogonal Matching Pursuit* (OMP) algorithm [29] for this work. This choice is due to its robustness and performance in the separation of signal components [27].

B. HARMONIC BASES DICTIONARIES

The construction of a dictionary suitable to the characteristics of the signals is significant to SSD performance [27]. The dictionary must be composed of analytical functions or parameterized waveforms containing the same characteristics of the signals. This dictionary supports the SSD in returning an appropriate sparse representation [23]. The stationary signals can have adequate sparse representations using *frequency dictionaries*, which can be represented by the Fourier dictionary.

The Fourier dictionary consists of atoms constructed from sine and cosine functions, according to the following equations:

$$\phi_{c,k} = \cos(\omega_k t) \quad \phi_{s,k} = \sin(\omega_k t). \tag{4}$$

The frequencies of each atom are calculated by $\omega_k = 2\pi k/N$, where $k = 0, \ldots, N/2$ for the cosine function and $k = 1, \ldots, N/2 - 1$ for the sine function. The default Fourier dictionary is complete ($M = N$) and its frequency resolution $\Delta_{f_{DFT}}$ is given by the ratio of the sampling frequency f_s and the number of signal samples (N). The default Fourier dictionary has $\Delta_{f_{DFT}} = 5$ Hz when it is respected

the signal sampling criterion defined in IEC 61000-4-7 [6]. This frequency resolution can be refined by assembling an overcomplete *Fourier dictionary*. This is achieved by letting $\omega_k = 2\pi k/(lN)$, where $k = 0, \ldots, (lN)/2$ for the cosine function and $k = 1, \ldots, (lN)/2 - 1$ for the sine function, and l is an integer greater than 1. This method is called *l-fold overcomplete system* and its frequency grid has resolution $\Delta_{f_{DFT}} = f_s/(lN)$ [26]. Each atom of the Fourier dictionary consists of complete cycles of cosines and sines. This feature allows the decomposition of stationary signals in components with integer multiple frequencies of $\Delta_{f_{DFT}}$.

The SSD of stationary signals can also be performed by dictionaries built by DTTs [26] which is the name given to the set of 16 transformations composed by eight DCTs (DCT-I to DCT-VIII), and eight DSTs (DST-I to DST-VIII) [30]. This variety of DCTs and DSTs results from different combinations of symmetry and edge conditions of their atoms [31]. Each atom can be symmetric or asymmetric at the initial and final limit points. The point of symmetry can be precisely on a sample (odd symmetry/anti-symmetry) or at the midpoint between two samples (even symmetry/anti-symmetry) [32]. Figure 1 illustrates the four possible cases.

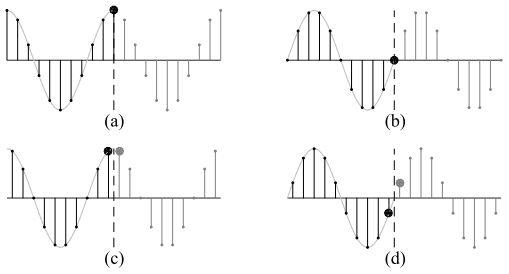

FIGURE 1. Examples of the symmetry types: (a) odd symmetry; (b) odd anti-symmetry; (c) even symmetry; and (d) even anti-symmetry [32]. The vertical line is the reference of the symmetry.

DCTs and DSTs from I to IV are known as *even* DTTs and are characterized by the symmetry point at both boundaries being similar (one sample or the center between two samples). The DCTs and DSTs from V to VII are called *odd* DTTs. These transforms have atoms with different points of symmetry at the boundaries [32]. The number of samples must match to DTT type [31]. The monitoring devices in power systems acquire the signals with 128, 256 or 512 samples per cycle [33]. Therefore, the odd DTTs are not suitable to decompose these signals. DCTs and DSTs from I to IV can decompose signals with an even number of samples in a period. Eqs. (5) and (6) build the atoms of these DTTs [31].

$$[\mathbf{DCT}_\beta]_{i\times j} = \sqrt{\frac{2}{N}}\,\varsigma \cos\left(\frac{(i+\Delta_i)\left(j+\Delta_j\right)\pi}{N}\right), \quad (5)$$

$$[\mathbf{DST}_\beta]_{i\times j} = \sqrt{\frac{2}{N}}\,\varsigma \sin\left(\frac{(i+\Delta_i)\left(j+\Delta_j\right)\pi}{N}\right), \quad (6)$$

where β is the type of DTT (I to IV), $\varsigma = 1$ except in the conditions shown in Table 1, i is the time variable, j is the frequency variable, and Δ indicates the time or frequency shift. These variables define the symmetry type of DTT, and the values adopted in each case are detailed in Table 1.

TABLE 1. Even DTT features [31].

	β	ς	Δ_i	Δ_j	i, j
DCT	I	$1/\sqrt{2}$, (if $i = 0$ or N) and ($j = 0$ or N)	0	0	$0, 1, \ldots, N$
	II	$1/\sqrt{2}$, if $j = 0$	1/2	0	$0, 1, \ldots, N-1$
	III	$1/\sqrt{2}$, if $i = 0$	0	1/2	$0, 1, \ldots, N-1$
	IV	1	1/2	1/2	$0, 1, \ldots, N-1$
DST	I	1	0	0	$1, 2, \ldots, N-1$
	II	$1/\sqrt{2}$, if $j = N-1$	1/2	1	$0, 1, \ldots, N-1$
	III	$1/\sqrt{2}$, if $i = N-1$	1	1/2	$0, 1, \ldots, N-1$
	IV	1	1/2	1/2	$0, 1, \ldots, N-1$

The frequency resolution $\Delta_{f_{DTT}}$ for all even DTTs is given by $f_s/(2N)$, which is twice the resolution obtained by DFT for signals with N samples. The frequency grid for each even DTT depends on the type of selected DTT because of the symmetry. Therefore, DCTs and DSTs can also be classified regarding the symmetry type of the atom in the frequency domain. Eq. (7) calculates the frequency grid for DCTs and DSTs of type I or II, while Eq. (8) calculates for type III or IV transforms [30].

$$f_{grid} = k\Delta_{f_{DTT}} \quad k = 1, 2, 3, 4, \ldots \quad (7)$$

$$f_{grid} = \left(k + \frac{1}{2}\right)\Delta_{f_{DTT}} \quad k = 1, 2, 3, 4, \ldots \quad (8)$$

Eq. (7) shows that the grid frequencies are multiples of $\Delta_{f_{DTT}}$ and match with the harmonics frequencies of the signals in the electrical systems. However, the atom frequencies in DTT dictionaries Type III or IV are shifted by $\Delta_{f_{DTT}}/2$. Consequently, the frequencies contained in this frequency grid do not match with the harmonic frequencies, which makes these DTTs unsuitable for decomposing harmonic components in electrical systems signals.

Although DCT-I and DST-I have the suitable frequency grid for signal of size N, the DST-I has odd asymmetry in both ends, which is implied in samples with the null value in the symmetry points [32], as can be observed in Figure 1b. Hence, the DST-I is suitable only for decomposing signals whose initial and final sample has a null value but is not suitable for harmonic analysis of phase-shifted signals. Accordingly, DCT-II and DST-II meet the appropriate conditions for analyzing signals with harmonic and interharmonic distortions: (I) processing an even number of samples; (II) the frequency grid of the atoms is composed by integer multiples of $\Delta_{f_{DTT}}$, which is the half of $\Delta_{f_{DFT}}$ for the same acquisition conditions; (III) meeting the requirements of even symmetry at both ends, which allows us to analyze phase-shifted signals.

C. DICTIONARY DESIGN

The dictionaries for this work have been built according to Eq. (9). We used DCT/DST pairs of the same type to ensure

suitable conditions of symmetry and frequency grid.

$$\Phi_\beta = \left[\mathbf{DCT}_\beta | \mathbf{DST}_\beta\right]. \tag{9}$$

The frequency resolution of the dictionary can be increased by using a *l-fold overcomplete system* [26]. Therefore, there are lN values in the frequency grid and Eqs. (5) and (6) are evaluated dividing the argument of the trigonometric functions by l. Thus, it is possible to reduce the interval in the frequency grid and to increase the range of frequencies available in the output spectrum. Thus, a more significant number of frequency components can be accurately estimated. Eq. (10) calculates the frequency resolution in this l-fold overcomplete dictionary,

$$\Delta_{f_{DTT}} = \frac{f_s}{2lN}. \tag{10}$$

The value of $\Delta_{f_{DTT}}$ reduces for integer values of $l > 1$. l can be adjusted according to the accuracy required in the harmonics and interharmonics estimation. Consequently, the number of atoms in the dictionary increases l times. The size of this overcomplete dictionary is $N \times 2\ lN$.

D. HIESSD ALGORITHM

The HIESSD algorithm can estimate harmonics and interharmonics components in the power system signals using different levels of resolution in the frequency grid. The HIESSD algorithm consists of two stages. In the *first stage*, the algorithm builds the overcomplete dictionary with the number of atoms suitable for the signal's characteristics. The *second stage* is responsible for estimating the harmonics and interharmonics components present in the signal. For this purpose, a sequence of steps is performed: (I) the decomposition of the signal to obtain the coefficients of the sparse vector; (II) the correction of these coefficients according to the characteristics of the dictionary used; (III) the calculation of the frequency components from these coefficients; (IV) and the application of a hard-threshold to drop the frequency components resulting from the noise in the signal.

The dictionary assembly needs the definition of these parameters: the type of DTT basis (β), the number of samples for the signal (N) and a scale-up factor to increase the resolution of the frequency grid (l). As shown in Section II-B, the DCT/DST II pair will be used, since it exhibits proper characteristics for this application. Therefore, β is set to II in Eqs. (5), (6) and (9). The amount of signal samples depends on the sampling frequency and the number of cycles of the signal to be analyzed. The choice of N and l influences the frequency resolution, and their values can be defined in order for $\Delta_{f_{DTT}}$ (Eq. (10)) to result in the desired resolution.

The second stage of the HIESSD algorithm starts after the assembly of $\mathbf{\Phi}$. The OMP algorithm works iteratively, operating on the following information [29]: (I) the iterations counter k; (II) the vector of sparse coefficients $\hat{\boldsymbol{\alpha}}$; (III) the residue $\mathbf{r}^k = (\mathbf{x} - \mathbf{\Phi}\hat{\boldsymbol{\alpha}})$; (IV) and set $\mathcal{S}^k$ which represents the solution support $\hat{\boldsymbol{\alpha}}$ (it contains the indices of the columns Φ which form the signal $\mathbf{x}$). At each iteration, the OMP algorithm searches in Φ the atom ϕ_m that results in the best approximation of the residue, which is done by calculating the inner product between the $\mathbf{r}^k$ and all atoms of the dictionary. The resulting index is stored in $\mathcal{S}^k$, and the coefficient related to that atom is calculated by $\hat{\boldsymbol{\alpha}}^{k+1} = \min_{\boldsymbol{\alpha}} \|\mathbf{x} - \mathbf{\Phi}_{\mathcal{S}^{k+1}}\hat{\boldsymbol{\alpha}}\|$. The coefficient value is put in $\hat{\boldsymbol{\alpha}}$, and $\mathbf{r}^{k+1}$ is updated. The process is repeated until the stop criterion $\|\mathbf{r}^k\| \leq \epsilon$ is reached. The value of ϵ is determined by the square root of the ratio between the variances of the noise and $\mathbf{x}$.

The OMP algorithm performs the decomposition of the signal $\mathbf{x}$ and returns the vector $\hat{\boldsymbol{\alpha}} = [\ \mathbf{c}\ |\ \mathbf{s}\ ]^T$, which contains the coefficients resulting from the sparse decomposition. The vectors $\mathbf{c} = [c_0, c_1, \ldots, c_{N-1}]^T$ and $\mathbf{s} = [s_1, s_2, \ldots, s_N]^T$ are related to the atoms of the matrices $\mathbf{DCT}_{II}$ and $\mathbf{DST}_{II}$, respectively. Each frequency component is formed by a parcel in c_j and another in s_j. However, these values cannot be used directly for estimating the frequency components, due to the time shift in DTT-II. The compensation of these coefficients should be carried out from the Eqs. (11) and (12). These equations are obtained by the substitution of Eqs. (5), (6) and (9) in (1), rearranging the terms on the right side of the equality and isolating time-dependent terms (i).

$$\Gamma_j = \sqrt{\frac{2}{N}}\left(c_j \cos\left(\frac{j\pi}{2N}\right) + s_j \sin\left(\frac{j\pi}{2N}\right)\right), \tag{11}$$

$$\Psi_j = \sqrt{\frac{2}{N}}\left(s_j \cos\left(\frac{j\pi}{2N}\right) - c_j \sin\left(\frac{j\pi}{2N}\right)\right). \tag{12}$$

After correcting the $\hat{\boldsymbol{\alpha}}$ coefficients, the amplitude A_j and the phase θ_j of each spectral component of $\mathbf{x}$ is respectively calculated by Eqs. (13) and (14)

$$A_j = \sqrt{\Gamma_j^2 + \Psi_j^2}, \tag{13}$$

$$\theta_j = \arctan\left(\frac{-\Psi_j}{\Gamma_j}\right). \tag{14}$$

The last step in the HIESSD algorithm is the removal of the influence of white Gaussian noise on the signal. This is achieved by applying a hard-threshold to the frequency components. The limit value τ used as the threshold is determined by employing the theorem known as near-minimaxity for upper-risk limits and known scale values [34], [35], according to Eq. (15). Therefore, only components with amplitude greater than τ are maintained, and the other components are dropped.

$$\tau = 2\sigma\frac{\sqrt{2\log(N)}}{\sqrt{N}}, \tag{15}$$

where σ is the standard deviation of the noise. Although the OMP algorithm already eliminates the most of the noise in the signal, the use of this threshold was necessary to remove some frequency components found by the OMP whose amplitude is close to the noise level. The structure of the HIESSD is displayed in the flowchart of Figure 2.

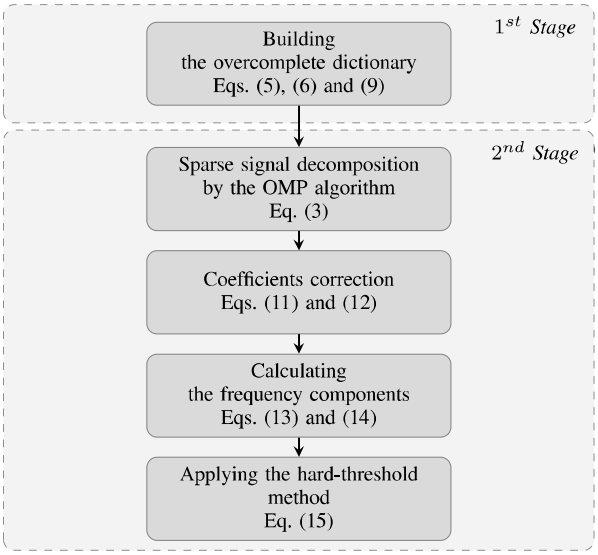

FIGURE 2. Struture of the HIESSD algorithm.

III. RESULTS

This section presents the evaluation of the performance of the HIESSD algorithm in estimating harmonics and interharmonics components of power systems signals. We compare these results with those obtained by processing the same signals using the DFT, MPM and FMP algorithms.

We assembled the overcomplete dictionary Φ as described in Section III-A, and each atom corresponds to sine and cosine components with frequencies from 0 Hz to 7680 Hz, in a grid with the frequency resolution of $2.5/l$ Hz. The HIESSD algorithm returns frequency, amplitude and phase information of each harmonic and interharmonic component present in the signal. We assess the quality of the estimates using the Mean Absolute Error (MAE) of each frequency component. The MAE is used for comparing methods under the following conditions: (I) signals not contaminated with noise; (II) signals in the presence of Gaussian white additive noise with signal-to-noise (SNR) ratios of 10, 20 and 40 dB; (III) different frequency grids using the *l-fold* method; and (IV) reduced signals sampling window. Initially, all signals tested have been sampled as recommended by IEC 61000-4-7 [6] with a 200 ms sampling window. The sampling rate has been set at 256 samples per cycle which results in a sampling frequency of 15360 Hz and $N = 3072$. The N and l parameters were altered for tests with a reduced sampling window.

The analyzed signals are typically in power system installations and contain only harmonic distortions or combine harmonics and interharmonics components. The results and discussions are presented in order of signal complexity: (I) over-excited transformer [36]; (II) single-phase DC source [37]; (III) three-phase inverter [38]; and (IV) synchronous machine [39].

A. ANALYSIS OF DICTIONARIES FORMED BY EVEN DTTS

Although the DCT-II/DST-II pair presents characteristics more suitable for decomposing power energy signals, one of the objectives of the present work is to assess how these signals are decomposed using dictionaries built from other even DTT pairs. We have used an electrical current signal with known harmonic distortion to evaluate the performance of the dictionaries formed by even DTT in the decomposition process. The signal used here is usually found in electrical distribution systems when the voltage level exceeds the nominal voltage values of a power transformer. This over-excitation causes an increase in the magnetizing current of the transformer and, consequently, harmonic distortion. The magnetizing current in a transformer with 30% of over-excitation is approximately 0.18 pu (per-unit) relative to the third harmonic and 0.11 pu referring to fifth harmonic [36]. Therefore, the test signal has been generated by the Eq. (16)

$$\mathbf{x}[n] = \sin(\omega n) - 0.18\sin(3\omega n) + 0.11\sin(5\omega n), \quad (16)$$

where $\omega = 2\pi 60\Delta_t$ for a power system in 60 Hz, Δ_t is the sampling time and $n = 0, 1, \ldots, N-1$. Following the requirements in IEC 61000-4-6 [6], the sampling window is 200 ms (12 full cycles of 60 Hz), and the sampling rate is 256 samples per cycle, resulting in Δ_t = 1/15360 s. The sparse decomposition has been performed using the OMP algorithm. Table 2 presents the results obtained applying the four possible dictionaries to estimate the harmonic components of the signal defined by Eq. (16).

TABLE 2. Frequency components resulting by decomposing the signal of Eq. (16) using Φ_I, Φ_{II}, Φ_{III} and Φ_{IV} with HIESSD algorithm.

Reference		Φ_I, Φ_{II} Estimation		Φ_{III}, Φ_{IV} Estimation	
Freq. (Hz)	Amp. (pu)	Freq. (Hz)	Amp. (pu)	Freq. (Hz)	Amp. (pu)
60	1.000	60	1.000	61.25	0.520
180	0.180	180	0.180	158.75	0.570
300	0.110	300	0.110	178.75	0.074
—	—	—	—	181.25	0.132
—	—	—	—	298.75	0.078
—	—	—	—	301.25	0.059

The frequency grids for Φ_I and Φ_{II} coincide with the exact frequencies in the signal. Consequently, the estimation of the frequency components is suitable using these dictionaries. When we have used Φ_{III} and Φ_{IV}, their frequency grids do not match the frequencies contained in the signal. Hence, the energy of each frequency component is distributed into the adjacent frequencies, resulting in estimation errors. Therefore, DCT/DST III and IV are not suitable for decomposing harmonic signals.

The process of analog-to-digital conversion typically uses sampling circuits based on *Phase-Locked-Loop* (PLL) technique, ensuring the beginning of the sampled signal always at the same phase [33]. Thus, all sampled signals have an exact number of full cycles, but the signal's phase is not guaranteed to be zero. Moreover, even if the sampled signal has phase zero; this does not mean that all the frequency components of the signal also have zero phase. Therefore, to evaluate the Φ_I and Φ_{II} regarding symmetry conditions,

the signal of the Eq. (16) has been modified by adding a phase of 30 degrees to each frequency component. In this new experiment, two factors have been evaluated to settle the quality of the decomposition process for each dictionary: (I) the residue between the reconstructed signal and the test signal; and (II) the accuracy of the frequency components.

Figure 3 shows the comparison between the test signal and the reconstructed signals by the coefficients obtained from Φ_I and Φ_{II}, and the residue of both reconstructions. Although the reconstructed signals do not have notable differences (Figure 3a), high values on the edges for the residue were observed when we used Φ_I (Figure 3b).

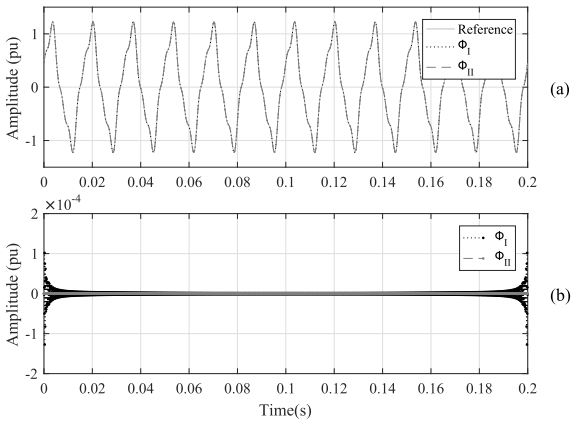

FIGURE 3. Comparison between the over-excited transformer current signal reconstruction from the coefficients obtained applying SSD method with Φ_I and Φ_{II}: (a) signal reconstructed; (b) residue.

When comparing the frequency components obtained by applying the decomposition using Φ_I and Φ_{II}, the results are even more apparent. The OMP algorithm has correctly identified all three frequency components of the signal when using the dictionary Φ_{II}. However, when using the dictionary Φ_I, the OMP algorithm has identified about 700 components. This is due to some frequency components of the signal being out of phase, and the initial and final samples of the signal are different from zero, while all atoms of Φ_I referred to DST have the initial and final samples equal to zero. Since, in this case, the signal is composed of sine components phase-shifted by 30 degrees, the OMP algorithm cannot match correctly the atoms of Φ_I to the signal's frequency components and, consequently, more atoms are needed to reduce the residual error. Figure 4 presents the frequency spectrum obtained for each dictionary. The high number of frequency components in signal's decomposition compromises the sparsity of the coefficient vector $\boldsymbol{\alpha}$, and the incorrect frequency and amplitude estimations of harmonic component make the spectral analysis for Φ_I unfeasible.

B. SINGLE-PHASE DC SOURCE

The use of nonlinear loads connected to the power system is the leading cause of distortions in current waveforms [37]. Power converters are examples of widely used nonlinear loads, causing the introduction of harmonic and

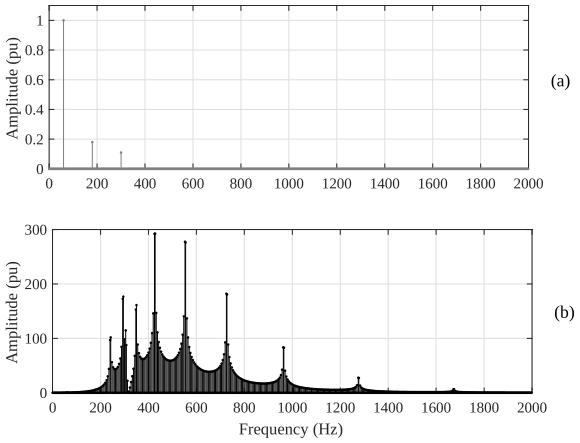

FIGURE 4. The frequency spectra of the over-excited transformer current signal resulting from the signal decomposition (a) using the dictionary Φ_2; and (b) using the dictionary Φ_1.

interharmonic components. Eq. (17) calculates the supply current from a DC source by an uncontrolled single-phase rectifier. The current signal of a DC source contains odd harmonics components with amplitudes inversely proportional to the harmonic order and alternating phases.

$$I_h = \begin{cases} +\dfrac{2\sqrt{2}}{h} I_{DC} & h = 1, 5, 9, 13, \ldots \\ -\dfrac{2\sqrt{2}}{h} I_{DC} & h = 3, 7, 11, 15, \ldots \\ 0 & h = 0, 2, 4, 6, \ldots \end{cases} \tag{17}$$

where I_{DC} is the maximum value of the current load. In this experiment, the signal from Eq. (17) has been used as the test signal, setting $I_{DC} = 1/(2\sqrt{2})$ to obtain normalized values.

As this signal has only frequency components that are integer multiples of the power system frequency, this signal can be easily decomposed into sines and cosines by DFT based methods when it is noise free. For this reason, we consider the DFT performance as the benchmark to be matched for this signal. However, signals sampled from real systems typically contain noise. Therefore, we added to the signal a white Gaussian noise with an SNR of 40 dB. The results of the decomposition of this signal by the HIESSD, DFT, MPM and FMP algorithms are shown in Table 3.

We observed that the performance of the HIESSD and DFT is similar for frequency, amplitude, and phase estimates, while MPM and FMP resulted in higher phase MAE for most estimated harmonics. Besides, FMP identified 485 components by using the same threshold value as in other methods. Meanwhile, the MPM identifies only the eight frequency components of the signal without the application of the hard-threshold. The HIESSD and DFT algorithms identified, respectively, 48 and 1537 components, requiring the application of the hard threshold to eliminate the frequency components that appear due to noise. However, these methods

TABLE 3. Estimations of the harmonic components of the supply current from a DC source added with a white Gaussian noise with SNR=40 dB. The harmonic components have been estimated by the HIESSD, MPM, DFT and FMP algorithms.

Reference			HIESSD				MPM				DFT				FMP			
			Estimation		MAE		Estimation		MAE		Estimation		MAE		Estimation		MAE	
Freq. (Hz)	Amp. (pu)	Phase (°)	Amp. (pu)	Phase (°)	Amp. (×0.001 pu)	Phase (°)	Amp. (pu)	Phase (°)	Amp. (×0.001 pu)	Phase (°)	Amp. (pu)	Phase (°)	Amp. (×0.001 pu)	Phase (°)	Amp. (pu)	Phase (°)	Amp. (×0.001 pu)	Phase (°)
60	1.000	-90	1.000	-90.02	0.000	0.02	0.999	-90.04	0.006	0.04	1.000	-90.02	0.000	0.02	1.000	-88.62	0.097	1.38
180	0.333	90	0.333	89.99	0.067	0.01	0.333	90.08	0.003	0.08	0.333	89.99	0.002	0.01	0.334	89.57	0.816	0.43
300	0.200	-90	0.200	-90.07	0.320	0.07	0.200	-90.28	0.016	0.28	0.200	-90.07	0.016	0.07	0.200	-91.03	0.298	1.03
420	0.143	90	0.143	89.99	0.229	0.01	0.143	89.77	0.010	0.23	0.143	89.97	0.016	0.03	0.143	91.05	0.006	1.05
540	0.111	-90	0.111	-89.96	0.067	0.04	0.111	-89.86	0.009	0.14	0.111	-89.95	0.008	0.05	0.111	-88.87	0.012	1.13
660	0.091	90	0.091	90.13	0.018	0.13	0.091	89.97	0.017	0.03	0.091	90.13	0.004	0.13	0.090	88.93	1.440	1.07
780	0.077	-90	0.077	-90.28	0.477	0.28	0.077	-89.97	0.042	0.03	0.077	-90.28	0.061	0.28	0.076	-90.02	0.795	0.02
900	0.067	90	0.067	90.29	0.121	0.29	0.066	90.95	0.084	0.95	0.067	90.29	0.017	0.29	0.067	92.65	0.031	2.65

TABLE 4. Performance of the HIESSD, MPM, DFT and FMP algorithms for estimating harmonic components in the current of a six-pulse three-phase rectifier on different conditions of noise. The symbol (*) indicates that the harmonic component was not estimated.

Reference		40 dB				20 dB				10 dB			
		HIESSD	DFT	MPM	FMP	HIESSD	DFT	MPM	FMP	HIESSD	DFT	MPM	FMP
Freq (Hz)	Amp. (pu)	Amp. (pu)	Amp. (pu)	Amp. (pu)	Amp. (pu)	Amp. (pu)	Amp. (pu)	Amp. (pu)	Amp. (pu)	Amp. (pu)	Amp. (pu)	Amp. (pu)	Amp. (pu)
60	1.000	1.000	1.000	1.000	1.001	0.999	0.999	1.003	1.005	1.010	1.010	1.002	0.995
300	0.187	0.186	0.186	0.186	0.185	0.189	0.189	0.190	0.184	0.186	0.186	(*)	0.181
420	0.124	0.124	0.124	0.124	0.124	0.124	0.124	0.121	0.126	0.124	0.124	(*)	0.115
660	0.064	0.064	0.064	0.064	0.064	0.065	0.065	(*)	0.066	0.059	0.060	(*)	0.073
780	0.046	0.046	0.046	0.046	0.046	0.045	0.045	(*)	0.047	0.034	0.034	(*)	0.048
1020	0.023	0.023	0.023	0.023	0.023	0.021	0.021	(*)	0.021	(*)	(*)	(*)	(*)
1140	0.015	0.015	0.015	0.016	0.015	0.016	0.017	(*)	0.019	(*)	(*)	(*)	(*)
1380	0.006	0.006	0.006	(*)	0.006	(*)	(*)	(*)	(*)	(*)	(*)	(*)	(*)
1500	0.005	0.005	0.005	(*)	0.006	(*)	(*)	(*)	(*)	(*)	(*)	(*)	(*)

also resulted in only eight frequency components when we have set $\tau = 0.0011$.

C. THREE PHASE INVERTER

Three-phase AC-DC converters are widely used in industrial facilities. A six-pulse three-phase rectifier generates harmonics components typically with frequency and amplitude given by Eq. (18)

$$\begin{aligned} h &= 6j \pm 1, \quad j = 1, 2, 3, \ldots, \\ I_h &= \frac{1}{h} I_1, \end{aligned} \tag{18}$$

where I_1 is the fundamental current. In [38], the authors presented a test signal which corresponds to the typical current in a six-pulse rectifier with a 10 degrees trigger angle. The signal's frequency components and the values estimated by the HIESSD, DFT, MPM and FMP algorithms (under varied noise conditions) are presented in Table 4.

The presence of components with minimal amplitude hinders the estimation process so that these components are not estimated. Considering $\tau = 0.0013$ for a noise with SNR = 40 dB, 0.011 for SNR = 20 dB and 0.034 for SNR = 10 dB, we can see that the HIESSD and DFT have estimated the frequency components limited by the value of τ. Meanwhile, the MPM have removed frequency components with the amplitude greater than τ. As we raised the noise level, some components were not estimated, increasing the inaccuracy of the results. Altough the FMP method identified the same frequency components as HIESSD and DFT algorithms, errors increased according to the noise level. In addition, FMP identified an average of 300 frequency components for SNR = 40 dB, 24 components for SNR = 20 dB and 27 components for SNR = 10 dB.

D. SYNCHRONOUS MACHINE

Synchronous machines are sources of interharmonic currents due to a non-sinusoidal variation of the mutual inductance of the rotor-stator assembly and of the unbalance in the rotor phase windings [39]. We have used the stator current signal defined in [39] to simulate this condition. The stator current signal is composed of the fundamental component in 60 Hz, two subharmonic components at 24 and 48 Hz, and five interharmonic components at 96, 264, 384, 588 and 708 Hz. These frequency values are not in the frequency grid of the DFT and HIESSD algorithms for $l = 1$.

However, when we set $l = 5$, the frequency resolution of the HIESSD increases to 0.5 Hz. Consequently, all frequency components of the stator current signal can be identified correctly. Figure 5a shows the real frequency spectrum of the test signal. The fundamental component (60 Hz) has been omitted for a better view. Figure 5b presents the interharmonics components estimated by the HIESSD. We do not recognize notable errors when compared to the real spectrum. Nevertheless, we can observe the *picket-fence* effect in the

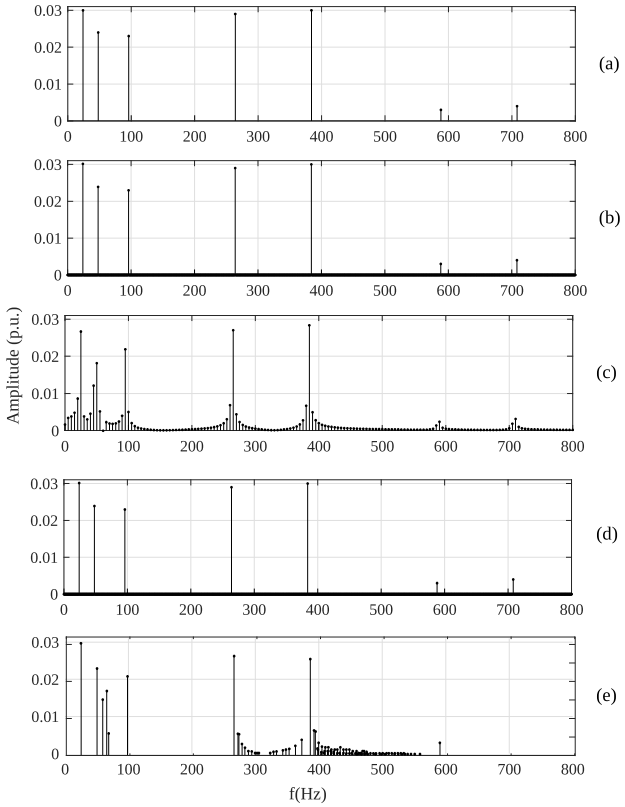

FIGURE 5. The estimated frequency spectra resulting from the signal decomposition of the stator current of a synchronous machine without noise. (a) Reference; (b) from the HIESSD with frequency resolution set to 0.5 Hz; (c) from the DFT; (d) from the MPM; (e) from the FMP.

spectrum estimated by the DFT algorithm which is displayed in Figure 5c. Energy scattering can be noticed in all interharmonics components. This effect hinders the identification of the frequency components. Figure 5d presents the spectrum estimated by MPM algorithm, which is similar to the result obtained by the HIESSD algorithm when no noise is present on the test signal. The FMP algorithm estimated 182 non-existent harmonics and interharmonics, as shown in Figure 5e.

Tuning the frequency resolution to 0.5 Hz increases the number of atoms by five times in the overcomplete dictionary, which increases the decomposition time of the signals. However, we have obtained suitable results setting the frequency resolution to 1 or 2 Hz. The resolution of the frequency grid was adjusted to 1 Hz by setting the sampling window to 166.67 ms and $l = 3$. We used a 125 ms sample window (7.5 full cycles) and $l = 2$ to set the frequency resolution to 2 Hz.

The results for estimating the harmonic and interharmonic components of the test signal with SNR = 40 dB using the HIESSD algorithm with frequency resolutions of 0.5, 1 and 2 Hz are shown in Table 5. We note that the results are similar, all frequency components are identified correctly, and the MAE in amplitude estimations are in the order of 10^{-4}. Table 6 also shows the results obtained by the MPM and FMP algorithms. The two smaller amplitude components are not identified by MPM, while the other components are estimated

TABLE 5. Frequency components estimation from the HIESSD algorithm for the stator current of a synchronous machine using different frequency resolution conditions.

Reference		Frequency resolution					
		0.5 Hz		1 Hz		2 Hz	
f (Hz)	Amp. (pu)	Amp. (pu)	MAE (pu)	Amp. (pu)	MAE (pu)	Amp. (pu)	MAE (pu)
24	0.0300	0.0301	0.0001	0.0299	0.0001	0.0299	0.0001
48	0.0240	0.0240	0.0000	0.0241	0.0001	0.0241	0.0001
60	1.0000	1.0000	0.0000	1.0000	0.0000	0.9999	0.0001
96	0.0230	0.0230	0.0000	0.0227	0.0003	0.0230	0.0000
264	0.0290	0.0290	0.0000	0.0291	0.0001	0.0290	0.0000
384	0.0300	0.0298	0.0002	0.0295	0.0005	0.0297	0.0003
588	0.0030	0.0032	0.0002	0.0029	0.0001	0.0028	0.0002
708	0.0040	0.0040	0.0000	0.0038	0.0002	0.0042	0.0002

with errors in frequency and amplitude in the order of 10^{-2} and 10^{-4}, respectively. The FMP algorithm identified the eight components, but with larger errors than MPM and also identified an average of 435 non-existent frequency components.

Comparing the results in Table 5 and Table 6, we can observe that the HIESSD algorithm estimates correctly all frequency components of the signal, while the MPM algorithm does not identify the two smaller components and the FMP estimated over 400 frequency components and the expected components presented larger errors than other methods. The threshold level adjusted at 0.001 pu for 40 dB in the HIESSD algorithm proved to be efficient because all components of the signal have been estimated without interference from the noise added to the signal. Because the MPM does not have a defined frequency grid, the frequency values of the components have small deviations from the exact value. The HIESSD algorithm is better than the MPM because it identifies all the frequency components of the signal correctly even with a high level of noise.

E. EXECUTION TIME

We implemented the HIESSD, DFT, MPM, and FMP algorithms using MATLAB software on a PC with AMD Phenom II X2 B55 3.0 GHz Processor. We measured the average execution time of each algorithm to estimate the frequency components for the signals of Sections III-B, III-C, and III-D, and the results are presented in Table 7.

The MPM algorithm presented the highest times of execution, followed by HIESSD, FMP, and DFT. HIESSD estimated accurately the real values of harmonics and interharmonics, estimating harmonics with results similar to the DFT and estimating interharmonics with results better than the DFT and FMP, which justifies its elevated execution time. In addition, the HIESSD algorithm presented better results than MPM, with a smaller execution time.

F. COMPARATIVE ANALYSIS

It was possible to observe the main advantages and disadvantages of each method. HIESSD and DFT work with a frequency grid, minimizing errors in frequency estimation

TABLE 6. Frequency components estimation from the MPM and FMP algorithms for the stator current of a synchronous machine. The symbol (*) indicates that the frequency component was not estimated.

Reference		MPM				FMP			
		Estimation		MAE		Estimation		MAE	
Freq. (Hz)	Amp. (pu)	Freq. (Hz)	Amp. (pu)	Freq. (Hz)	Amp. (pu)	Freq. (Hz)	Amp. (pu)	Freq. (Hz)	Amp. (pu)
24	0.030	24.02	0.0296	0.02	0.0004	23.82	0.0301	0.18	0.0001
48	0.024	48.03	0.0240	0.03	0.0000	48.36	0.0235	0.36	0.0005
60	1.000	60.00	0.9997	0.00	0.0003	59.93	1.0020	0.07	0.0020
96	0.023	95.98	0.0227	0.02	0.0003	96.29	0.0216	0.29	0.0014
264	0.029	263.99	0.0289	0.01	0.0001	263.80	0.0261	0.20	0.0029
384	0.030	383.99	0.0297	0.01	0.0003	384	0.0284	0.00	0.0016
588	0.003	(*)	(*)	(*)	(*)	588.30	0.0035	0.30	0.0005
708	0.004	(*)	(*)	(*)	(*)	708.10	0.0042	0.10	0.0002

TABLE 7. Average execution times for estimating frequency components.

Algorithm	Sect. III-B	Sect. III-C			Sect. III-D
	40 dB	40 dB	20 dB	10 dB	l=5, 40 dB
HIESSD	4.50 s	3.75 s	3.44 s	3.00 s	5.64 s
MPM	9.26 s	6.57 s	7.42 s	17.1 s	15.2 s
DFT	0.33 s	0.25 s	0.27 s	0.62 s	0.44 s
FMP	2.35 s	1.95 s	0.28 s	0.73 s	4.97 s

when compared to MPM and FMP. The spectrum resolution can be improved in HIESSD by changing the fold. This is not possible in DFT since its grid is fixed, which implies in its high susceptibility to spectral leakage. On the other hand, MPM and FMP do not work with frequency grids, which can result in significant errors in estimating frequency values. MPM could not identify components with a small amplitude, and FMP identified nonexistent components, depending on the value set for tolerance. However, the advantages of HIESSD are reflected in its high runtime over DFT and FMP.

IV. CONCLUSION

We have presented in this paper the HIESSD method, which is an algorithm for the estimation of harmonics and interharmonics components of power system signals based on the sparse decomposition from an overcomplete dictionary. The choice of this overcomplete dictionary was based on the evaluation of all possible DTTs. From the tests carried out with the even DTTs, the pair DCT/DST-II has presented more satisfactory results due to the suitable frequency grid and the robustness concerning the edge conditions of the signals. As in the DFT method, the HIESSD algorithm uses a fixed frequency grid to calculate the frequency spectrum of a signal. The frequency values of this grid are adjusted by applying the l-fold technique, which makes it possible to increase the frequency resolution of the grid without changing the signal acquisition conditions. This procedure allows the estimation of interharmonic components with increased accuracy.

We have compared the performance of the HIESSD algorithm with three different techniques: DFT, MPM, and FMP. The HIESSD algorithm has presented better results than the DFT in the estimation of interharmonics, due to the frequency resolution setting, and similar results for harmonics estimation. The HIESSD has been shown more robustness to noise than the MPM and FMP and had better results when we reduced the sampling window size. We will proceed this work in the future by including impulsive atoms to the overcomplete dictionary and the frequency deviation analysis. Hence, we look forward to characterizing power quality disturbances such as transients, notches, sags, and swells.

ACKNOWLEDGMENT

The authors would like to thank UTFPR, CAPES, Fundação Araucária, FINEP, and CNPq for scholarships and additional funding.

REFERENCES

[1] H. C. Lin, "Identification of interharmonics using disperse energy distribution algorithm for flicker troubleshooting," *IET Sci., Meas. Technol.*, vol. 10, no. 7, pp. 786–794, Sep. 2016, doi: 10.1049/iet-smt.2016.0110.

[2] A. Testa *et al.*, "Interharmonics: Theory and modeling," *IEEE Trans. Power Del.*, vol. 22, no. 4, pp. 2335–2348, Oct. 2007, doi: 10.1109/TPWRD.2007.905505.

[3] *IEEE Recommended Practice and Requirements for Harmonic Control in Electric Power Systems*, IEEE Standard 519-2014, Jun. 2014, pp. 1–29, doi: 10.1109/IEEESTD.2014.6826459.

[4] D. Kumar, F. Zare, and A. Ghosh, "DC microgrid technology: System architectures, AC grid interfaces, grounding schemes, power quality, communication networks, applications, and standardizations aspects," *IEEE Access*, vol. 5, pp. 12230–12256, 2017, doi: 10.1109/ACCESS.2017.2705914.

[5] S. K. Singh, N. Sinha, A. Kumar, and G. N. Sinha, "Robust estimation of power system harmonics using a hybrid firefly based recursive least square algorithm," *Int. J. Elect. Power Energy Syst.*, vol. 80, pp. 287–296, Sep. 2016, doi: 10.1016/j.ijepes.2016.01.046.

[6] *Electromagnetic Compatibility (EMC)—Part 4-7: Testing and Measurement Techniques–General Guide on Harmonics and Interharmonics Measurements and Instrumentation, for Power Supply Systems and Equipment Connected Thereto*, Standard IEC 61000-4-7, 2006.

[7] C. Li, W. Xu, and T. Tayjasanant, "Interharmonics: Basic concepts and techniques for their detection and measurement," *Electr. Power Syst. Res.*, vol. 66, no. 1, pp. 39–48, Jul. 2003, doi: 10.1016/S0378-7796(03)00070-1.

[8] L. Feola, R. Langella, I. Papic, and A. Testa, "Selective interharmonic compensation to improve Statcom performance for light flicker mitigation," *IEEE Trans. Power Del.*, vol. 33, no. 5, pp. 2442–2451, Oct. 2018, doi: 10.1109/TPWRD.2018.2810333.

[9] E. Durna, I. Yilmaz, and M. Ermiş, "Suppression of time-varying interharmonics produced by medium-frequency induction melting furnaces by a HAPF system," *IEEE Trans. Power Electron.*, vol. 32, no. 2, pp. 1030–1043, Feb. 2017, doi: 10.1109/TPEL.2016.2542140.

[10] H. C. Lin, "Development of interharmonics identification using enhanced-FFT algorithm," *J. Eng.*, vol. 2017, no. 7, pp. 333–342, Jul. 2017, doi: 10.1049/joe.2017.0133.

[11] Z. Sun, Z. He, T. Zang, and Y. Liu, "Multi-interharmonic spectrum separation and measurement under asynchronous sampling condition," *IEEE Trans. Instrum. Meas.*, vol. 65, no. 8, pp. 1902–1912, Aug. 2016, doi: 10.1109/TIM.2016.2562278.
[12] P. D. Achlerkar, S. R. Samantaray, and M. S. Manikandan, "Variational mode decomposition and decision tree based detection and classification of power quality disturbances in grid-connected distributed generation system," *IEEE Trans. Smart Grid*, vol. 9, no. 4, pp. 3122–3132, Jul. 2018, doi: 10.1109/TSG.2016.2626469.
[13] K. Dragomiretskiy and D. Zosso, "Variational mode decomposition," *IEEE Trans. Signal Process.*, vol. 62, no. 3, pp. 531–544, Feb. 2014, doi: 10.1109/TSP.2013.2288675.
[14] K. Sheshyekani, G. Fallahi, M. Hamzeh, and M. Kheradmandi, "A general noise-resilient technique based on the matrix pencil method for the assessment of harmonics and interharmonics in power systems," *IEEE Trans. Power Del.*, vol. 32, no. 5, pp. 2179–2188, Oct. 2017, doi: 10.1109/TPWRD.2016.2625329.
[15] A. F. Rodríguez, L. D. S. Rodrigo, E. L. Guillén, J. M. R. Ascariz, J. M. M. Jiménez, and L. Boquete, "Coding Prony's method in MATLAB and applying it to biomedical signal filtering," *BMC Bioinf.*, vol. 19, no. 1, Nov. 2018, Art. no. 451, doi: 10.1186/s12859-018-2473-y.
[16] M. Mohanty, U. Satija, B. Ramkumar, "Sparse decomposition framework for maximum likelihood classification under alpha-stable noise," presented at the IEEE Int. Conf. Electron., Comput. Commun. Technol. (CONECCT), Jul. 2015, doi: 10.1109/CONECCT.2015.7383931.
[17] R. Demirli and J. Saniie, "Model-based estimation pursuit for sparse decomposition of ultrasonic echoes," *IET Signal Process.*, vol. 6, no. 4, pp. 313–325, Jun. 2012, doi: 10.1049/iet-spr.2011.0093.
[18] Q. Xie, Y. Wang, T. Li, X. Bian, H. Zhang, and Y. Xu, "Application of signal sparse decomposition in the detection of partial discharge by ultrasonic array method," *IEEE Trans. Dielectr. Electr. Insul.*, vol. 22, no. 4, pp. 2031–2040, Aug. 2015, doi: 10.1109/TDEI.2015.004955.
[19] G. Dong, G. Kuang, N. Wang, L. Zhao, and J. Lu, "SAR target recognition via joint sparse representation of monogenic signal," *IEEE J. Sel. Topics Appl. Earth Observ. Remote Sens.*, vol. 8, no. 7, pp. 3316–3328, Jul. 2015, doi: 10.1109/JSTARS.2015.2436694.
[20] J. Wang, M. She, S. Nahavandi, and A. Kouzani, "Human identification from ECG signals via sparse representation of local segments," *IEEE Signal Process. Lett.*, vol. 20, no. 20, pp. 937–940, Oct. 2013, doi: 10.1109/LSP.2013.2267593.
[21] U. Satija, B. Ramkumar, and S. Manikandan, "Noise-aware dictionary-learning-based sparse representation framework for detection and removal of single and combined noises from ECG signal," *Healthcare Technol. Lett.*, vol. 4, no. 1, pp. 2–12, Feb. 2017, doi: 10.1049/htl.2016.0077.
[22] Y. Li, Z. L. Yu, N. Bi, Y. Xu, Z. Gu, and S.-I. Amari, "Sparse representation for brain signal processing: A tutorial on methods and applications," *IEEE Signal Process. Mag.*, vol. 31, no. 3, pp. 96–106, May 2014, doi: 10.1109/MSP.2013.2296790.
[23] M. S. Manikandan, S. R. Samantaray, and I. Kamwa, "Simultaneous denoising and compression of power system disturbances using sparse representation on overcomplete hybrid dictionaries," *IET Gener., Transmiss. Distrib.*, vol. 9, no. 11, pp. 1077–1088, Aug. 2015, doi: 10.1049/iet-gtd.2014.0806.
[24] M. S. Manikandan, S. R. Samantaray, and I. Kamwa, "Detection and classification of power quality disturbances using sparse signal decomposition on hybrid dictionaries," *IEEE Trans. Instrum. Meas.*, vol. 64, no. 1, pp. 27–38, Jan. 2015, doi: 10.1109/TIM.2014.2330493.
[25] L. Chen, D. Zheng, S. Chen, and B. Han, "Method based on sparse signal decomposition for harmonic and inter-harmonic analysis of power system," *J. Electr. Eng. Technol.*, vol. 12, no. 2, pp. 559–568, Mar. 2017, doi: 10.5370/JEET.2017.12.2.559.
[26] S. Shaobing, D. L. Donoho, and M. A. Saunders, "Atomic decomposition by basis pursuit," *SIAM Rev.*, vol. 43, no. 1, pp. 129–159, 2001, doi: 10.1137/S003614450037906X.
[27] Z. Feng, Y. Zhou, M. J. Zuo, F. Chu, and X. Chen, "Atomic decomposition and sparse representation for complex signal analysis in machinery fault diagnosis: A review with examples," *Measurement*, vol. 103, pp. 106–132, Jun. 2017, doi: 10.1016/j.measurement.2017.02.031.
[28] J. A. Tropp and S. J. Wright, "Computational methods for sparse solution of linear inverse problems," *Proc. IEEE*, vol. 98, no. 6, pp. 948–958, Jun. 2010, doi: 10.1109/JPROC.2010.2044010.
[29] M. Elad, *Sparse and Redundant Representations: From Theory to Applications in Signal and Image Processing*. New York, NY, USA: Springer, 2010.
[30] Z. Wang and B. R. Hunt, "The discrete *W* transform," *Appl. Math. Comput.*, vol. 16, no. 1, pp. 19–48, Jan. 1985, doi: 10.1016/0096-3003(85)90008-6.
[31] V. Britanak, P. C. Yip, and K. R. Rao, *Discrete Cosine and Sine Transforms: General Properties, Fast Algorithms and Integer Approximations*. Oxford, U.K.: Academic, 2007, ch. 1, pp. 1–15.
[32] S. A. Martucci, "Symmetric convolution and the discrete sine and cosine transforms," *IEEE Trans. Signal Process.*, vol. 42, no. 5, pp. 1038–1051, May 1994, doi: 10.1109/78.295213.
[33] *IEEE Recommended Practice for Monitoring Electric Power Quality*, IEEE Standard 1159-2009, Jun. 2009, doi: 10.1109/IEEESTD.2009.5154067.
[34] D. L. Donoho, I. M. Johnstone, G. Kerkyacharian, and D. Picard, "Wavelet shrinkage: Asymptopia?" *J. Roy. Stat. Soc., B (Methodol.)*, vol. 57, no. 2, pp. 301–369, 1995, 10.2307/2345967.
[35] D. L. Donoho, I. M. Johnstone, G. Kerkyacharian, and D. Picard, "Universal near minimaxity of wavelet shrinkage," in *Festschrift for Lucien Le Cam*, D. Pollard, E. Torgersen, and G. L. Yang, Eds. New York, NY, USA: Springer, 1997, pp. 183–220.
[36] J. Arrillaga and N. R. Watson, *Power System Harmonics*. Chichester, U.K.: Wiley, 2003, pp. 1–15.
[37] M. H. J. Bollen and I. Y.-H. Gu, *Signal Processing of Power Quality Disturbances*. Hoboken, NJ, USA: Wiley, 2006.
[38] D. E. Rice, "A detailed analysis of six-pulse converter harmonic currents," *IEEE Trans. Ind. Appl.*, vol. 30, no. 2, pp. 294–304, Mar./Apr. 1994, doi: 10.1109/28.287531.
[39] A. K. Wallace, E. S. Ward, and A. Wright, "Sources of harmonic currents in slip-ring induction motors," *Proc. Inst. Electr. Eng.*, vol. 121, no. 12, pp. 1495–1500, Dec. 1974, doi: 10.1049/piee.1974.0312.

TATIANA DE ALMEIDA PRADO received the B.S. degree in electrical engineering from the State University of Western Paraná (Unioeste), Foz do Iguaçu, Brazil, in 2005, and the M.Sc. degree in electrical engineering from Universidade Tecnológica Federal do Paraná (UTFPR), Câmpus Pato Branco, Brazil, in 2019. She is currently pursuing the Ph.D. degree with UTFPR, Câmpus Curitiba, Brazil. Her research interests include power quality and ultrasonic non-destructive inspections (NDT).

ANDRÉA MACARIO BARROS received the B.S. degree in electrical engineering from Universidade Tecnológica Federal do Paraná (UTFPR), Câmpus Pato Branco, Brazil, where she is currently pursuing the M.Sc. degree. Her research interests include power quality and methods for harmonics and interharmonic estimation.

GIOVANNI ALFREDO GUARNERI received the B.S. degree in electrical engineering, the M.Sc. and Ph.D. degrees in electrical engineering and industrial informatics from Universidade Tecnológica Federal do Paraná (UTFPR), Câmpus Curitiba, Brazil, in 1992, 1996, and 2015, respectively. Since 2007, he has been with the Electrical Engineering Department, UTFPR, Câmpus Pato Branco, Brazil. His current research interests include signal processing in electrical power systems and ultrasonic non-destructive inspections (NDT).